

## Article

# Pharmacophore Modeling and Binding Affinity of Secondary Metabolites from *Angelica keiskei* to HMG Co-A Reductase

Diah Lia Aulifa <sup>1,2,\*</sup> , Siti Rafa Amirah <sup>1</sup> , Driyanti Rahayu <sup>1</sup> , Sandra Megantara <sup>1</sup>  and Muchtaridi Muchtaridi <sup>1</sup> 

<sup>1</sup> Department of Pharmaceutical Analysis and Medicinal Chemistry, Faculty of Pharmacy, Universitas Padjadjaran, Jl. Raya Bandung-Sumedang Km. 21, Bandung 45363, Indonesia; siti19001@mail.unpad.ac.id (S.R.A.); driyanti.rahayu@unpad.ac.id (D.R.); s.megantara@unpad.ac.id (S.M.); muchtaridi@unpad.ac.id (M.M.)

<sup>2</sup> Study Center for Development of Pharmaceutical Preparations, Universitas Padjadjaran, Jl. Raya Bandung-Sumedang Km. 21, Bandung 45363, Indonesia

\* Correspondence: diah.lia@unpad.ac.id

**Abstract:** Statins are cholesterol-lowering drugs with a mechanism of inhibiting 3-hydroxy-3-methylglutaryl-CoA reductase, but long-term use can cause side effects. An example of a plant capable of reducing cholesterol levels is *Angelica keiskei* (ashitaba). Therefore, this study aimed to obtain suitable compounds with inhibitory activity against the HMG-CoA reductase enzyme from ashitaba through in silico tests. The experiment began with screening and pharmacophore modeling, followed by molecular docking on ashitaba's compounds, statins groups, and the native ligand was (3R,5R)-7-[4-(benzyl carbamoyl)-2-(4-fluorophenyl)-5-(1-methylethyl)-1H-imidazole-1-yl]-3,5-dihydroxyheptanoic acid (4HI). Based on the results of the molecular docking simulations, 15 hit compounds had a small binding energy ( $\Delta G$ ). Pitavastatin, as the comparator drug ( $\Delta G = -8.24$  kcal/mol;  $K_i = 2.11$   $\mu\text{M}$ ), had a lower  $\Delta G$  and inhibition constant ( $K_i$ ) than the native ligand 4HI ( $\Delta G = -7.84$  kcal/mol;  $K_i = 7.96$   $\mu\text{M}$ ). From ashitaba's compounds, it was found that 4'-O-geranylningenin, luteolin, isobavachalcone, dorsmannin A, and 3'-carboxymethyl-4,2'-dihydroxy-4'-methoxychalcone have low  $\Delta G$  of below  $-6$  kcal/mol. The lowest  $\Delta G$  value was found in 3'-carboxymethyl-4,2'-dihydroxy-4'-methoxy chalcone with a  $\Delta G$  of  $-6.67$  kcal/mol and  $K_i$  value of  $16.66$   $\mu\text{M}$ , which was lower than the  $\Delta G$  value of the other comparator drugs, atorvastatin ( $\Delta G = -5.49$  kcal/mol;  $K_i = 1148.17$   $\mu\text{M}$ ) and simvastatin ( $\Delta G = -6.50$  kcal/mol;  $K_i = 22.34$   $\mu\text{M}$ ). This compound also binds to the important amino acid residues, including ASN755D, ASP690C, GLU559D, LYS735D, LYS691C, and SER684C, through hydrogen bonds. Based on the results, the compound effectively binds to six important amino acids with good binding affinity and only requires a small concentration to reduce half of the enzyme activity.

**Keywords:** statins; HMG-CoA reductase; *Angelica keiskei*; in silico



check for updates

**Citation:** Aulifa, D.L.; Amirah, S.R.; Rahayu, D.; Megantara, S.; Muchtaridi, M. Pharmacophore Modeling and Binding Affinity of Secondary Metabolites from *Angelica keiskei* to HMG Co-A Reductase. *Molecules* **2024**, *29*, 2983. <https://doi.org/10.3390/molecules29132983>

Academic Editor: Armando Zarrelli

Received: 31 May 2024

Accepted: 18 June 2024

Published: 23 June 2024



**Copyright:** © 2024 by the authors. Licensee MDPI, Basel, Switzerland. This article is an open access article distributed under the terms and conditions of the Creative Commons Attribution (CC BY) license (<https://creativecommons.org/licenses/by/4.0/>).

## 1. Introduction

Cholesterol is a waxy, fat-like substance found in all cells within the body, specifically the liver [1]. The presence of excess levels in the bloodstream is a major contributor to plaque formation, which can clog the arteries thus causing heart attacks [2]. A crucial enzyme in cholesterol biosynthesis is 3-hydroxy-3-methylglutaryl (HMG) Co-A reductase, which catalyzes the conversion of HMG-CoA to mevalonic acid [3]. Statins are cholesterol-lowering drugs commonly used by the public due to their efficacy as inhibitors of the HMG-CoA reductase enzyme [4]. Statins have proven potential in reducing LDL levels by 20–60% [5–8]. Statins are divided into two groups, namely lipophilic and hydrophilic statins. Bitzur et al., 2013, proved that lipophilic statins, including simvastatin and atorvastatin, tend to cause myopathy compared to hydrophilic statins; in addition, long-term use potentially causes side effects, including [9], hepatotoxicity, and increased risk of new-onset type 2 diabetes [10]. As stated in the previous studies, statins could increase the risk of

developing diabetes mellitus (DM), but the results have not been statistically significant. In contrast, the West of Scotland Coronary Prevention Study (WOSCOPS) trial showed that statins, specifically pravastatin [11] and pitavastatin [12], have the potential to reduce the risk of diabetes.

Empirically, one of the herbal plants used to reduce cholesterol levels is ashitaba [13]. *Angelica keiskei* (Miq.) Koidzumi, commonly known as ashitaba or Japanese celery, originates from Japan but can be cultivated in Indonesia, specifically in the Mojokerto and Lombok regions. Compounds isolated from ashitaba include various types of chalcones [14–25], flavonoids [16,24], and coumarins [23,24]. Previous studies have also reported the presence of sesquiterpenes [26], diterpenes [27], triterpenes [27,28], and various other compounds [23,24,27,28]. According to an in vivo study by Zhang et al., 2015, administration of the ashitaba extract (0.01% and 0.1%, *w/w*) for 16 weeks, containing 4-hydroxyderricin and xanthoangelol, effectively suppressed weight gain, as well as reduced plasma cholesterol, glucose, and insulin levels. The treatment increased adiponectin levels, while also reducing triglycerides and liver cholesterol levels in C57BL/6 rats [29]. Moreover, dry extracts of the stems and leaves have been used in health and cosmetic products at a safe dose of approximately 300 mg/kg [13].

Along with technological developments, the discovery and development of new drug candidates classified as complex can be relatively shorter with in silico tests [30]. It is a computational method used in drug design that provides convenience by shortening the process of identifying hit compounds, as well as the selection of hit-to-lead compounds, and prevents problems related to side effects from the drugs being developed [31]. Therefore, this study aimed to carry out an in silico test to determine the inhibitory activity of the active compounds in the ashitaba plant compared with the statin groups (approved by FDA) (Supplementary S1) against the HMG-CoA reductase enzyme using pharmacophore modeling methods and docking simulations.

## 2. Results

### 2.1. Visualization Results of the HMG-CoA Reductase Pharmacophore Feature

Pharmacophore modeling was conducted using two methods, namely structure-based drug designing (SBDD) and ligand-based drug designing (LBDD). In the SBDD method, the target protein used as a structural basis was HMG-CoA reductase (PDB ID: 3CCW) complexed with a native ligand (3R,5R)-7-[4-(benzyl carbamoyl)-2-(4-fluorophenyl)-5-(1-methylethyl)-1H-imidazole-1-yl]-3,5-dihydroxy heptanoic acid (C<sub>27</sub>H<sub>31</sub>N<sub>3</sub>O<sub>5</sub>F<sub>1</sub>) or 4HI. This ligand has good pharmacophore features and compatibility with Lipinski's rules, possessing nine hydrogen bond acceptors, two hydrogen bond donors, four hydrophobic interactions, one negative and zero positive ionized areas (Figure 1), as well as a molecular weight of 496.56 g/mol, and cLogP of 0.80. The results suggest that the pharmacophore features were present in one molecule recognized by the receptor site and are responsible for the biological activity of the compounds.

Ligand-based pharmacophore modeling was carried out using 299 active compounds (actives) HMG-CoA reductase inhibitors and 8884 inactive compounds (decoys) downloaded from the DUD-E (A Database of Useful Decoys). From the results, 10 models were obtained with the pharmacophore features including 2 hydrogen bond acceptors, 1 hydrogen bond donor, and 1 hydrophobic interaction. Figure 2 shows the visualization of the essential features of a ligand-based pharmacophore with biological effects on the target.

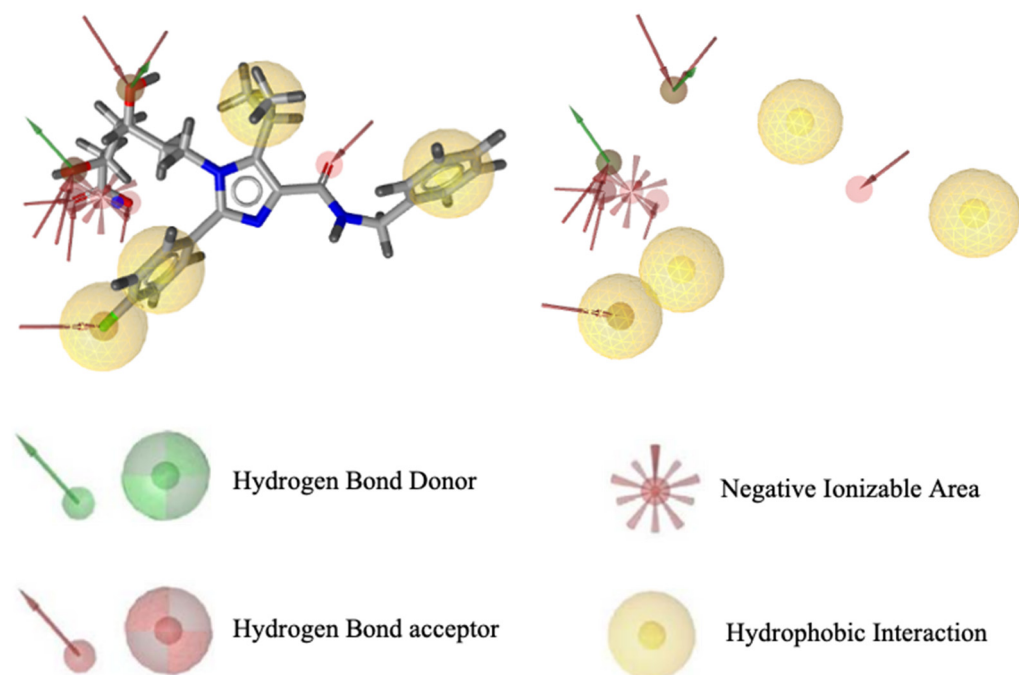


**Figure 1.** Visualization of pharmacophore features based on HMG-CoA reductase structure.

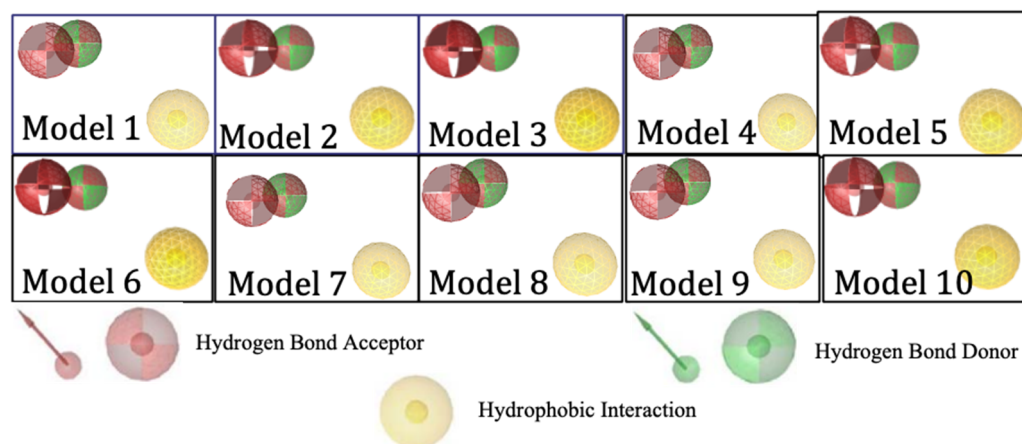


**Figure 2.** Visualization of ligand-based pharmacophore features.

## 2.2. The Pharmacophore Model Validation Results

The pharmacophore model needs to be validated before being used as a reference in virtual screening. This step aims to ensure the ability of the pharmacophore model to distinguish between active and inactive compounds. Pharmacophore validation was carried out using 1 structure-based and 10 ligand-based pharmacophore models.

Figure 3 shows the ROC curve from the result of a plot between true positive (sensitivity) on the Y-axis and false positive (1-specificity) on the X-axis in the best model, namely ligand-based model 7. The area under the ROC curve (Figure 3) was in the range of zero to one or 0–100%. The higher the area under the curve, the better the prediction of the model for active compounds than the decoy [32].

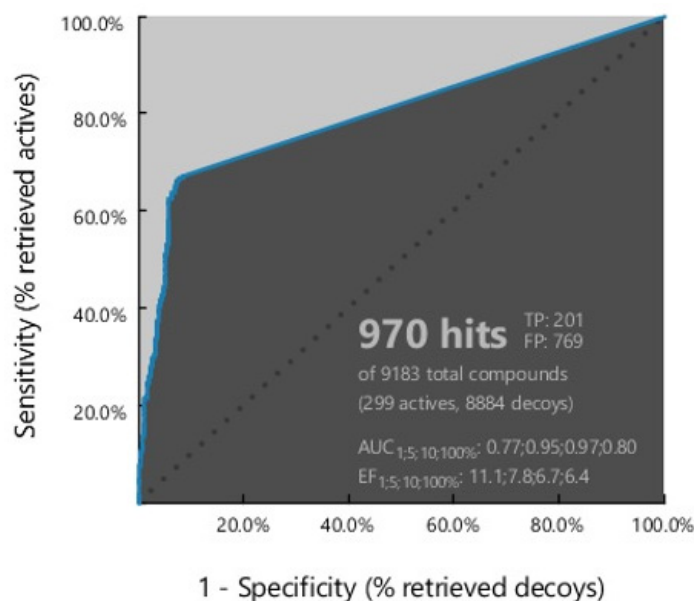


**Figure 3.** ROC validation curve.

Model 7 recognized 970 hits with an AUC value of 0.8, an EF value of 6.4, and a GH score of 0.3. The best model selected had a partial area under the curve (pAUC) value of 0.77, 0.95, and 0.97 at 1%, 5%, and 10%, respectively. In addition, this model was sensitive, identifying 201 active compounds out of 209, representing 67% of the total active compounds. The high selectivity and sensitivity indicate that the pharmacophore model is an excellent filter for recognizing HMG-CoA reductase inhibitors. All model validation parameters shown in Table 1 suggest the good quality of the pharmacophore model for the screening stage of hit compounds.

**Table 1.** Pharmacophore Modeling Validation Parameters.

Parameter	Result
Total compounds in database (D)	9183
Active total in database (A)	299
Total hits (Ht)	970
Active hits (Ha)/True Positive (TP)	201
False Positives (FP)	769
True Negatives (TN = D – FP)	8414
False Negatives (FN = A – Ha)	98
Area Under ROC Curve (AUC)	0.8
Enrichment Factor (EF = [Ha × D]/[Ht × A])	6.4
Goodness of Hit score (GH = $[\frac{Ha(3A+Ht)}{4HtA}] \{1 - \frac{(Ht-Ha)}{(D-A)}\}$ )	0.3
Sensitivity (TPR = TP/A)	0.67
Specificity (TNR = TN/D)	0.92
Accuracy (ACC = (TP + TN)/(A + D))	0.91

### 2.3. Hit Compound Screening Results

Table 2 showed that 15 out of 36 hit compounds had the highest pharmacophore fit scores. The screening was carried out using a database of tests and standards with a validated pharmacophore model through Ligandscout. These 15 hit compounds were then molecularly docked to HMG-CoA reductase (PDB:3CCW) using the AutoDockTools-1.5.6 software.

**Table 2.** Pharmacophore Screening Result.

No.	Compound	Fit-Pharmacophore Score (%)
1	4HI	47.05
2	Pitavastatin	48.14
3	Atorvastatin	48.07
4	Lovastatin	47.55
5	Simvastatin	47.44
6	Mevastatin (Compactin)	47.39
7	4'-O-Geranylaringenin	47.98
8	Luteolin	47.70
9	Cynaroside	47.47
10	7-O-Methyl prostratol F	47.40
11	Xanthokeismin A	47.31
12	Daucosterol	46.92
13	Isobavachalcone	46.92
14	Dorsmannin A	46.91
15	3'-Carboxymethyl-4,2'-dihydroxy-4'-methoxy chalcone	46.90
16	Xanthokeistal A	46.71

#### 2.4. The Results of Molecular Docking Validation

The validation of the molecular docking or redocking was carried out between the prepared native ligand and the target protein, namely 3CCW, to identify and ascertain the location of the binding site on the enzyme. The size of the grid box used was  $40 \times 40 \times 40 \text{ \AA}$  to ensure sufficient space to search for the best position of the ligand on the binding site. An overly large grid box size can lead to non-specific ligand binding and biased test results. The coordinates used were x (3.788), y (30.858), and z (5.445), particularly for positioning the ligand in the active pocket of the HMG-CoA reductase receptor. From this process, an RMSD value of  $0.98 \text{ \AA}$  was obtained, indicating that the molecular docking method met the qualifications and showed good quality of bond pose reproduction because the RMSD value was less than  $2.00 \text{ \AA}$  (Figure 4) [33,34]. The native ligand 4HI binds to the important amino acids ARG590C, ASN755D, ASP690C, and SER565D. It also binds to other amino acids including ALA856D, ASN658C, CYS561D, GLY560D, HIS752D, and LEU853D. In the native ligand, the result of re-docking showed an  $\Delta G$  of  $-7.84$  with a  $K_i$  value of  $7.96 \text{ \mu M}$ .

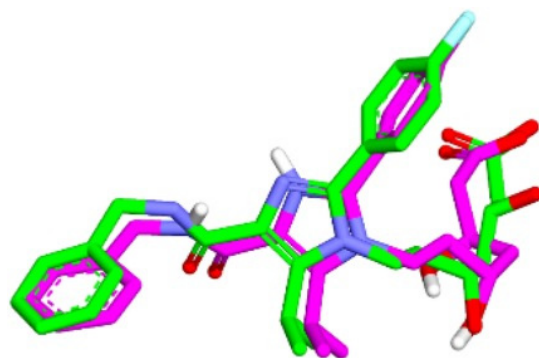


**Figure 4.** Overlaying of extracted 4HI molecules from HMG-CoA reductase (Green) with re-docking (Pink) (RMSD =  $0.98 \text{ \AA}$ ).

### 2.5. The Molecular Docking Result of Hit Compounds to HMG-CoA Reductase

Molecular docking was carried out to determine the possible interactions between the hit test compounds and important amino acid residues of the target enzyme HMG-CoA reductase in the body compared to native ligands and marketed comparators. The amino acid residues crucial to the catalytic site of the HMG-CoA reductase enzyme according to Sarver et al., 2008, include GLU559, SER565, ARG590, SER684, ASP690, LYS691, LYS735, and ASN755 through hydrogen bonding [7]. This was also supported by Istvan et al., 2001, stating that important amino acids were in the cis loop area, including GLU559, ARG590, SER684, ASP690, LYS691, LYS692, LYS735, and ASN755 [35]. The molecular docking used the grid box arrangement obtained in the validation process to center the test ligands with the active sites on the native ligands. Among the 100× dockings performed, the conformation of the best cluster and the lowest bond energy was selected.

The lowest bond affinity ( $\Delta G$ ) value was found in 3'-carboxymethyl-4,2'-dihydroxy-4'-methoxy chalcone, which is lower than the  $\Delta G$  value of the comparator drugs atorvastatin and simvastatin. This compound also binds to the important amino acid residues including ASN755D, ASP690C, GLU559D, LYS735D, LYS691C, and SER684C through hydrogen bonds. Pitavastatin, as the comparator drug, had a lower  $\Delta G$  and inhibition constant than the native ligand.

### 3. Discussion

The process of cholesterol synthesis begins with the condensation of two molecules of acetyl-coenzyme A (acetyl-CoA) to form the intermediate acetoacetyl-CoA, catalyzed by acetyl-CoA acetyltransferase (thiolase enzyme). Furthermore, the reaction of two acetoacetyl-CoA molecules allows the formation of 3-hydroxy-3-methylglutaryl CoA (HMG-CoA) catalyzed by HMG-CoA synthase, then the reduction to mevalonate by the enzyme HMG-CoA reductase (two molecules of NADPH serve as cofactors). These reactions are the rate-limiting steps of the body's overall cholesterol synthesis and are known as regulatory enzymes [6,36]. Istvan and colleagues successfully performed crystallographic analysis on the catalytic site of human HMGR, a tetramer form, which is composed of two dimers having two active sites (first dimer: monomer 1 $\alpha$  and 1 $\beta$ ; second dimer: monomer 2 $\alpha$  and 2 $\beta$ ). They also revealed that the catalytic monomer of hHMGR consists of three domains as follows: N-domain (in N-terminal; residues 460–525; helices L $\alpha$ 1-5), a large L-domain (residues 528–590 and 694–872; helices L $\alpha$ 1-11 and L $\beta$ 1-6) and a small S-domain (residues 592–682; helices S $\alpha$ 1-3 and S $\beta$ 1-4). The S and L domains are connected by strands, L $\beta$ 3 and S $\beta$ 1, and a loop (residues 682–694; known as a 'cis-loop') that is important in the HMG binding site [36]. On the other hand, Costa and colleagues studied the conformational changes of HMGR in complex with HMG-CoA (binds L $\alpha$ 1-domain; amino acid 528–590) and NADPH (binds S-domains) by constructing a model of human HMGR (hHMGR), which comprised ligand-free hHMGR (Apo form), hHMGR complexed with HMG-CoA and NADPH (holo form), and phosphorylated hHMGR. Their study also found that the L2-domain located with the HMG-CoA binding region on the B chain does not interact with substrates and cofactors [37].

Statins are drugs that can bind well to the active side of the HMG-CoA reductase enzyme to inhibit the interaction of the enzyme with the substrate. There is some disagreement regarding the use of statins as anti-cholesterol drugs to increase the occurrence of diabetes. Atorvastatin and simvastatin have an increased risk of DM compared to pravastatin [38]. Still, Cho et al., 2015 [11], reported that there was no significant difference in the risk of T2DM between hydrophilic (pravastatin and rosuvastatin) and lipophilic (simvastatin, atorvastatin, and pitavastatin) statins. The structure and bioavailability of statins do not significantly impact the diabetogenic effect, which is a condition of increased glucose production through carbohydrate/glucose metabolism [11]. Sarver et al., 2008, succeeded in synthesizing imidazole compound 1 (4HI), which has good in vivo efficacy as an inhibitor with an IC<sub>50</sub> of 7.9 nM and excellent hepatoselectivity (>1000-fold). This compound, which is complex with HMG-CoA reductase, was crystalized with X-ray diffraction

and deposited in rcsb.org (accessed on 3 February 2023). (PDB ID: 3CCW) and used in this study [7].

In this study, we used a pharmacophore modeling approach with the two models namely, the SBDD and LBDD methods [6]. In the SBDD method, the target protein used as a structural basis was HMG-CoA reductase (PDB ID: 3CCW). This ligand has good pharmacophore features and compatibility with Lipinski's rules, possessing nine hydrogen bond acceptors, two hydrogen bond donors, four hydrophobic interactions, one negative and zero positive ionized areas, as well as a molecular weight of 496.56 g/mol, and cLogP of 0.80. The results suggest that the pharmacophore features were present in one molecule recognized on a receptor site and responsible for the biological activity of compounds.

In the discovery of new compounds, it is necessary to use active compounds and decoy compounds in a ratio of 1:10 [39,40]. Ligand-based pharmacophore modeling was conducted using 299 active compounds (actives) of HMG-CoA reductase inhibitors and 8884 inactive compounds (decoys) downloaded from the DUD-E database (A Database of Useful Decoys) [41]. The DUD-E site already stores data on active compounds which are compounds that are proven to have activity against HMG-CoA reductase enzymes, so they can be used as positive controls. Conversely, decoy compounds are compounds in nature that do not have biological activity against the HMG-CoA reductase enzyme, so they are used as negative controls [40,42]. Pharmacophore validation was carried out using 1 structure-based and 10 ligand-based pharmacophore models. The higher the area under the curve, the better the prediction of the model for active compounds than decoy [32]. The best model, namely ligand-based model 7, was sensitive in identifying 201 active compounds out of 209, representing 67% of the total active compounds. The high selectivity and sensitivity indicate that the pharmacophore model is an excellent filter for recognizing HMG-CoA reductase inhibitors.

All statins are good competitor inhibitors of HMG-CoA reductase because they have pharmacophore groups that show great similarity to the HMG-CoA molecule [43]. Markowska et al., 2020, suggested that statins that have a hydroxy acid form in the side group (pravastatin, atorvastatin, cerivastatin, fluvastatin, pitavastatin, and rosuvastatin) are predicted to have pharmacological activity, while the lactone form in the side group of statins (mevastatin, lovastatin, and simvastatin) could reduce pharmacological activity [8]. Different results appear in this study, based on pharmacophore study, and showed that 36 hit compounds (9 statins and 27 ashitaba's compounds) had pharmacophore fit scores. This shows that ligand-based model 7 could recognize the active compound (all statins) on the HMG-CoA reductase receptor. We selected 15 compounds (5 statins and 10 ashitaba's compounds; >46% pharmacophore-fit scores) for molecular docking (Table 2). Pitavastatin and atorvastatin, which have a hydroxy acid form, are hit compounds (fit-pharmacophore results of 48.14% and 48.07%, respectively); however, compounds which have lactone sides such as lovastatin, simvastatin, and mevastatin (compactin) are included in the hit compounds as well (fit-pharmacophore results of 47.55%; 47.44%, and 47.39%), based on pharmacophore screening results.

The molecular docking parameter in this study is the affinity energy/binding energy ( $\Delta G$ ). Binding energy shows the energy required to bind two molecules; the smaller the energy required to bind to the target protein, the more effective it is. The second parameter is the  $K_i$  value. This is a semi-empirical free energy constant usually indicates the inhibition of receptors in micromolar units ( $\mu\text{M}$ ), which virtually explores the dose concentration. The calculation of the inhibition constant ( $K_i$ ) value is obtained from the binding energy ( $\Delta G$ ) using the following formula:  $K_i = \exp(\Delta G/RT)$ , where  $R$  is the universal gas constant ( $1.985 \times 10^{-3} \text{ kcal mol}^{-1} \text{ K}^{-1}$ ) and  $T$  is the temperature (298.15 K). Thereafter, we analyzed the interaction between ligands and receptors at coordinates  $x = 3.788$ ;  $y = 30.858$ ; and  $z = 5.445$ . The expected interaction is the ligand with key amino acids on the receptor that plays a role in providing biological activity. Amino acid residues which play a role in the catalytic site of the HMG-CoA reductase enzyme, according to Sarver et al., 2008, include GLU559, SER565, ARG590, SER684, ASP690, LYS691, LYS735, and ASN755 through

hydrogen bonding [7]. This was also supported by Istvan et al., 2001, who has crystalized six statins with X-ray diffraction and studied the mechanism. They found that when HMG-CoA or CoA substrates are bound to amino acid residues, the C-terminal extension is partially fixed. Still, when the NADP<sup>+</sup>, HMG, and CoA or NADP<sup>+</sup> and HMG-CoA substrates are complexed together, the helix at the C-terminal of L $\alpha$ 11 (residues 870 and 871) binds to the protein core (known as the cis loop) [36,44]. This configuration would cause the active site to be closed by the L $\alpha$ 11 helix, and no statins would be able to occupy the NADP(H) binding site, which is a finding that is in line with their kinetic studies, as statins are competitive inhibitors of HMG-CoA substrates but are not competitive with NADPH [35,36]. The important amino acids were in the cis loop area, including GLU559, ARG590, SER684, ASP690, LYS691, LYS692, LYS735, and ASN755 (with polar interaction, hydrogen bonding, forming a salt bridge and hydrophobic interaction) [35]. Istvan et al., 2001, also stated that hydrophobic statin compounds with a large molecular weight can occupy the surface of the HMG-CoA binding pocket, causing the substrate of HMG-CoA to HMGR to be blocked [35]. Van der Waals bonds are also formed between the hydrophobic side chains, namely the amino acids LEU562, VAL683, LEU853, ALA856, and LEU857 with statins and ashitaba's compounds [35].

In this research, the native ligand 4HI binds to the important amino acids ARG590C, ASN755D, ASP690C, and SER565D. It also binds to other amino acids including ALA856D, ASN658C, CYS561D, GLY560D, HIS752D, and LEU853D. For the native ligand (4HI), the result of re-docking showed an  $\Delta G$  of  $-7.84$  with a  $K_i$  value of  $7.96 \mu\text{M}$ . Based on the results of molecular docking simulations, 15 hit compounds had a small binding energy ( $\Delta G$ ). Pitavastatin, as the comparator drug, ( $\Delta G = -8.24$  kcal/mol;  $K_i = 2.11 \mu\text{M}$ ) had lower  $\Delta G$  and inhibition constant ( $K_i$ ) than the native ligand 4HI. From ashitaba's compounds, we found that the compounds 4'-O-Geranylaringenin, luteolin, isobavachalcone, dorsmanin A, and 3'-Carboxymethyl-4,2'-dihydroxy-4'-methoxy chalcone have a low  $\Delta G$  below  $-6$  kcal/mol (Table 3). The lowest  $\Delta G$  value was found in 3'-carboxymethyl-4,2'-dihydroxy-4'-methoxy chalcone with a  $\Delta G$  of  $-6.67$  kcal/mol and  $K_i$  value of  $16.66 \mu\text{M}$ , which was lower than the  $\Delta G$  value of the comparator drugs atorvastatin ( $\Delta G = -5.49$  kcal/mol;  $K_i = 1148.17 \mu\text{M}$ ) and simvastatin ( $\Delta G = -6.50$  kcal/mol;  $K_i = 22.34 \mu\text{M}$ ). This compound also binds to the important amino acid residues including ASN755D, ASP690C, GLU559D, LYS735D, LYS691C, and SER684C through hydrogen bonds (Figure 5). Based on the results, the compound effectively binds to six important amino acids with good binding affinity and only requires a small concentration to reduce half of the enzyme activity.

**Table 3.** Molecular docking results of the hit compounds.

No.	Compound	$\Delta G$ (kcal/mol)	$K_i$ ( $\mu\text{M}$ )	Important Amino Acid Residues [7]	Other Amino Acid Residues
<b>Reference Drugs</b>					
1	Pitavastatin	$-8.24$	2.11	ARG590C, ASN755D, ASP690C, GLU559D, LYS691D, SER565D	LEU562D, LYS692C, HIS752D, LEU853D, ALA856D
2	Atorvastatin	$-5.49$	1148.17	ARG590C, GLU559D, LYS735D, SER684C	CYS561D, ALA564D, LEU853D
3	Lovastatin	$-6.88$	10.65	ARG590C, ASP690C, LYS691C	LEU562D, HIS752D, LEU853D, ALA856D
4	Simvastatin	$-6.50$	22.34	ARG590C, ASP690C, LYS735D, SER684C	SER661C, VAL683C, LYS692C, HIS752D, LEU853D, LEU857D
5	Mevastatin (Compactin)	$-6.86$	11.82	ARG590C, LYS691C, SER565D	CYS561D, LEU562D, MET657C, LEU853D, LEU857D

Table 3. Cont.

No.	Compound	$\Delta G$ (kcal/mol)	$K_i$ ( $\mu M$ )	Important Amino Acid Residues [7]	Other Amino Acid Residues
<b>Ashitaba's Compounds</b>					
1	4'-O-Geranylningenin	-6.48	20.24	ARG590C, ASN755D, ASP690C, LYS691C, SER684C	CYS561D, LEU562D, ASN686C, ALA751D, HIS752D, LEU853D, ALA856D
2	Luteolin	-6.03	40.69	ASP690C, GLU559D, LYS735D, SER565D, SER684C	LEU562D, ALA751D, HIS752D, LEU853D
3	Cynaroside	-5.43	153.65	ARG590C, ASP690C, ASN755D, GLU559D	LYS692C, ALA751D, LEU853D, ALA856D
4	7-O-Methyl prostratol F	-5.84	70.70	ASN755D, ASP690C, GLU559D, LYS735D, LYS691C, SER684C	CYS561D, CYS688C, HIS752D, LEU853D
5	Xanthokeismin A	-5.11	202.71	ARG590C, ASN755D, ASP690C, LYS691C, SER565D, SER684C	CYS561D, LEU562D, VAL683C, LEU853D, ALA856D, LEU857D
6	Daucosterol	-5.41	203.28	ARG590C, ASN755D, ASP690C, GLU559D, LYS735D, LYS691C	CYS561D, ALA564D, ALA751D, ALA856D, LEU853D
7	Isobavachalcone	-6.00	42.71	ARG590C, ASP690C, GLU559D, LYS691C, SER565D	MET657C, ALA751D, SER852D, LEU853D, ALA856D
8	Dorsmannin A	-6.65	15.78	ARG590C, ASP690C	CYS561D, LEU562D, LEU853D, ALA856D
9	3'-Carboxymethyl-4,2'-dihydroxy-4'-methoxy chalcone	-6.67	16.66	ASN755D, ASP690C, GLU559D, LYS735D, LYS691C, SER684C	CYS561D, CYS688C, HIS752D, LEU853D
10	Xanthokeistal A	-4.77	487.55	ASP690C, LYS691C, SER565D	CYS561D, LYS692C, ALA751D, HIS752D, LEU853D, ALA856D

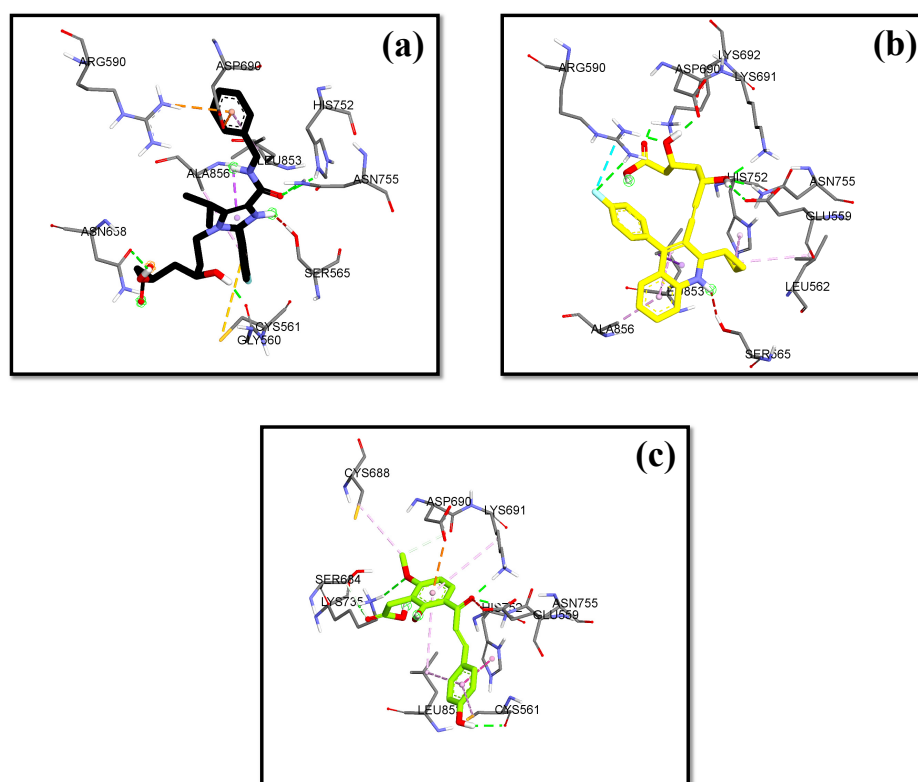


**Figure 5.** HMG Co-A reductase binding mode with (a) 4HI (b) Pitavastatin (c) 3'-carboxymethyl-4,2'-dihydroxy-4'-methoxy chalcone.

The C-terminal region (residue 870–886), Flap domain, was involved in the open-closed movement of the active site [37]. In humans, HMGR activity can be modulated by

phosphorylation. If phosphorylation occurs at residue 872, close to the important catalytic residue 866, it can reduce protein activity. Istvan's finding that the position of residue 872 is around the  $\alpha$ -phosphate of NADP and the side chain of residue 871, not close to residue 866. Phosphorylation can cause a decrease in affinity for NADPH [36]. Our docking results showed that neither the statins nor/or ashitabas's compounds bind to residues 870–872 at the C-terminus, so neither statins nor ashitaba's compounds may be competitive with NADPH.

In this study, we conducted the predictions of physicochemical properties for 15 hit compounds by screening Lipinski's rule of five (RO5). The RO5 bases pharmacokinetic drug properties such as absorption, distribution, metabolism, and excretion on certain physicochemical properties [45]. A compound can be used as a drug compound if it has a molecular mass of less than 500 Daltons because the molecular weight parameter is related to the polymer chemical properties of the compound. A high polymer molecular weight indicates stronger polymer chemical properties. In addition, it is also related to the compound distribution process, because compounds with molecular weights of more than 500 Da cannot passively diffuse so in penetrating biological membranes, the absorption of compounds in the body becomes longer [46,47]. Second, the partition coefficient ( $\log P$ ) should be less than five. A large  $\log P$  value indicates that the compound is hydrophobic and tends to have a high level of toxicity, retained longer in the lipid bilayer, and distributed more widely in the body so that the compound's affinity to the enzyme is reduced. A negative  $\log P$  value would make it difficult for the compound to pass through the lipid bilayer membrane [48], which allows for rapid interaction of the molecule with the water solvent [47]. Finally, the number of hydrogen bond donors should be less than 5, and hydrogen bond acceptors should be less than 10. This was because the higher the hydrogen bond capacity, the higher the energy required in the absorption process, so that the ability of the hydrogen bond acceptor is reduced [48]. The physicochemical profiles of compounds would be similar across industries if the testing methodology, selection criteria, and compounds screened were similar. The results of Lipinski's rule of five analysis on 15 compounds (Supplementary S2) that fit the pharmacophore modeling could provide data on the physicochemical properties of these compounds, which may be useful in subsequent in vitro or in vivo testing. We conduct this RO5 as a tool to guide early-stage drug discovery.

## 4. Materials and Methods

### 4.1. Instruments

The tools used in computational testing include hardware and software with different functions and purposes. The hardware comprised a personal laptop with AMD A9-9420e Radeon R5 processor specifications, 5 computer cores 2C + 3G 1.80 GHz; 8.00GB RAM; system type 64 bit, x64-based processor; and Windows 10 Pro version 22H2 operating system. On the other hand, software was obtained free of charge for academic users. These included the following: LigandScout 4.4.5 (IntelLigand, <https://ligandscout.software.informer.com/>, Vienna, Austria; accessed on February–May 2023) for pharmacophore modeling and screening. AutoDockTools-1.5.6 (The Scripps Research Institute, <http://autodock.scripps.edu/>), Command Prompt, and Notepad-11.2307.27.0 were used for ligand and receptor preparation, validation, as well as molecular docking simulations. The BIOVIA Discovery Studios 2021 Client (Dassault Systems Biovia, <https://discover.3ds.com/discovery-studio-visualizer-download>) was used for the preparation of receptors with native ligands, to visualize the results of complex molecular docking, bonding between ligands and receptors, geometrical optimization, and overlays in the validation process. Moreover, ChemDraw Ultra 12.0 (PerkinElmer Inc., <http://www.cambridgesoft.com/>) was used to draw the 2D structures of the ligand compounds. Chem3D Pro 12.0 (PerkinElmer Inc., <http://www.cambridgesoft.com/>) was used to convert the 2D structure ligand into a 3D shape and optimize the energy. Open Babel-2.4.1 (Open Babel community <http://openbabel.org/docs/Installation/install.html>) was used to convert chemical file formats,

while the DUD-E site accessed on <https://dude.docking.org/> was used to get active and decoy databases. The NCBI site, accessed at <https://www.ncbi.nlm.nih.gov/>, was used to search for recorded test compounds. The Protein Data Bank site accessed at <https://www.rcsb.org/structure/3CCW> was used to search for the target receptor code and SwissADME at <http://www.swissadme.ch/index.php> was utilized for the prediction of physicochemical properties.

#### 4.2. Materials

The materials used in this study included the three-dimensional structure of the target receptor resulting from an X-ray crystallographic depiction of the HMG-CoA reductase enzyme in the Homo sapiens/human organism (PDB ID: 3CCW), with a good resolution of 2.10 Å downloaded through the Protein Data Bank (<http://www.rcsb.org/>, accessed on January–May 2023). Molecular docking validation was carried out using the BIOVIA Discovery Studios 2021 Client. The ligand used as a positive control/reference drug was the three-dimensional structure of (3R,5R)-7-[4-(benzyl carbamoyl)-2-(4-fluorophenyl)-5-(1-methylethyl)-1H-imidazole-1-yl]-3,5-dihydroxyheptanoic acid (4HI), which was separated from the target protein using the BIOVIA Discovery Studios 2021 Client program, as well as the statins (Supplementary S1) available on the market. In addition, the tested ligands used were two-dimensional structures of 115 secondary metabolites isolated from ashitaba plant, namely 42 chalcones, 7 flavanones, 3 flavones, 5 flavonols, 39 coumarins, 2 phenolics, 3 sesquiterpenes, 1 diterpene, 3 triterpenes, and 12 other compounds obtained by preparation using the ChemDraw Ultra 12.0 and Chem3D Pro 12.0.

#### 4.3. Methods

This study was carried out using the *in silico* (computation-based) method, with initial stages including modeling, validation, and pharmacophore screening using LigandScout 4.4.5. Other steps were molecular docking simulations, prediction of pharmacokinetic properties and ligand toxicity, as well as reviewing the achievement of Lipinski's Rule of Five (RO5).

#### 4.4. Pharmacophore Modeling

Pharmacophore modeling was carried out through the Structure-Based Drug Design (SBDD) and Ligand-Based Drug Design (LBDD) methods. Structure-based pharmacophore modeling was conducted by opening and then resetting LigandScout 4.4.5 first to the default settings. In the 'Structure-Based' section, the 3D structure of the HMG-CoA reductase target protein with the 3CCW PDB code was downloaded. Following this, the 'Create Pharmacophore' icon was clicked until the pharmacophore features of the native ligands were visible to the target protein.

In the ligand-based pharmacophore modeling, the material needed during the prepared test included three databases, namely active, decoy, and test compounds. The database was made by opening the LigandScout 4.4.5 program and clicking the 'Ligand Based' column. Active/decoy files obtained from the DUD-E website were opened for the active/decoy database, while for the test database, the test compound was opened to be tested and optimized in 3D form. In the 'Type' section, all compounds were in the 'training' form for active and decoy databases, while for the database, all compounds were in the 'Test' form. The files were stored in the LDB format, and the pharmacophore modeling stage was continued after all databases were deemed ready.

In the 'Ligand Based' section of the active database previously opened, the cluster was made on all compounds, then the sequence of compounds was 'sorted by cluster'. This was achieved by clicking the 'Cluster ID' column, and one type of 'training' file was selected from each cluster. The 'Create Pharmacophore' icon was clicked, and 10 pharmacophore models were stored in the PMZ format.

#### 4.5. Pharmacophore Validation

The pharmacophore model previously obtained was tested for validity by moving to the 'Screening' column by clicking the 'Copy to Other Perspective', and then the 'Screening Perspective' icon. In the 'Screening' column, 'Load Screening Database' was clicked to select the active and decoy database with the LDB format previously created. The active database entered was marked in green, while the decoy was marked in red. The 'Perform Screening' icon was clicked to allow LigandScout 4.4.5 to perform the screening process. To visualize the validity of the 'Plot ROC Curve', the AUC value was observed, and then the best ROC and EF from the 10 models were selected.

#### 4.6. Screening of Hit Compounds

In the 'Screening' column, 'Load Screening Database' was clicked to select the test database of the test compound previously created. The database is marked in green and in the 'Ligand Based' section, the best model was moved to the 'Screening' column. The 'Perform Screening' icon was then clicked to derive a hit compound.

#### 4.7. Molecular Docking Simulation

##### 4.7.1. Separation of Native Ligands and Receptors

The HMG-CoA Reductase enzyme as macromolecules (receptors) originating from humans, with the PDB code 3CCW, was downloaded on the bank data protein website (<https://www.rcsb.org/>, accessed on January–May 2023). The receptors were cleaned from other components not needed in docking protocols, including water molecules and ligands using BIOVIA Discovery Study 2021 Client (<https://discover.3ds.com/discovery-studio-visualizer-download>, accessed on May–July 2023) and saved to the PDB format. This step was also carried out to separate the native ligands from the macromolecules.

##### 4.7.2. Ligand Preparation

The ligand structure was designed by opening the ChemDraw Ultra 12.0 to form 113 structures of the compound from ashitaba and on ChemACX.Com, accessed on January–May 2023). Structural modification was carried out by adding or removing according to the structure source of compounds on the NCBI site or the reference literature, and the file was then stored in a CDX format. Furthermore, 2D structures/images were converted to 3D, followed by the minimization of energy (MM2) using the Chem3D Pro 12.0 to obtain a more stable structure. The files were stored in the PDB format. Autodock Tools-1.5.5 was used to edit the PDB format ligand by adding hydrogen atoms then selecting 'Merge Non-Polar', computing Gasteiger charge, and adding torsion. The files were stored in the PDBQT format.

##### 4.7.3. Macromolecule Preparation

Macromolecule preparation was performed using Autodock Tools-1.5.5, followed by editing the receptor file in a PDB format by adding hydrogen and then selecting 'Polar Only' and Kollman charge. The files were stored in the PDBQT format. To determine the binding site ligand in the receptor, the grid parameter was determined using Autodock Tools-1.5.6. The receptors were selected as macromolecules, and the 'map type' was set by selecting ligands. The search for active site receptors was carried out by clicking 'Center on Ligand' to obtain the size of the Center Grid Box (X, Y, and Z). This size must be used in adjusting between the active side of the receptor and other ligands. The files were stored in the GPF (Grid Parameter File) format.

##### 4.7.4. Molecular Docking

PDBQT format receptors were first designated as macromolecules, then as ligands for the docking process. Docking was performed using the Lamarckian GA (Genetic Algorithm) with parameters set for 100 runs, followed by adjustment to the default docking parameter, and files were then stored in the DPF (Docking Parameter File) format. Further-

more, the molecular docking process was carried out using the Command Prompt feature. Determination of the ligand conformation with the results of the best molecular docking was conducted by selecting ligand conformation with the lowest bond energy level. Free binding energy values and RMSD were derived from the histogram in the DLG format docking file using Notepad. The conformations were then made into a complex file in PDB format. Complex files were visualized using the BIOVIA Discovery Studio 2021 Client to observe the overlay display of re-docking results and ligand interactions with receptors in 2D or 3D diagrams. Docking visualization is needed to find out the locations of the ligand and the receptor. In addition to visualizing the inhibited side, visualization also helps avoid errors in the docking process.

#### 4.7.5. Overview of Lipinski's Rule of Five (RO5)

Lipinski's Rule of Five (RO5) was conducted to guide early-stage drug discovery. Predictions of the physicochemical properties were conducted online on the SwissADME website (<http://www.swissadme.ch/index.php>, accessed on January–May 2023). The candidates for active compounds in the drugs should comply with Lipinski's five rules, namely molecular weight  $\leq 500$ , hydrogen bonds acceptor  $\leq 10$ , hydrogen bond donors  $\leq 5$ , and logP value  $\leq 5$  (or MlogP  $\leq 4.15$ ) [49].

## 5. Conclusions

In conclusion, for the native ligand (4HI), the result of re-docking showed a  $\Delta G$  of  $-7.84$  with a  $K_i$  value of  $7.96 \mu\text{M}$ . Based on the results of molecular docking simulations, 15 hit compounds had a small binding energy ( $\Delta G$ ). Pitavastatin, as the comparator drug, had lower  $\Delta G$  and  $K_i$  values than the native ligand 4HI. The best docking result of ashitaba's compound, 3'-carboxymethyl-4,2'-dihydroxy-4'-methoxy chalcone has one hydrophobic interaction, one hydrogen bond donor, and two hydrogen bond acceptors based on modeling with a pharmacophore fit score of 46.90%. This compound also had six hydrogen interactions with the important amino acid residues, ASN755D, ASP690C, GLU559D, LYS735D, LYS691C, and SER684C, with a  $\Delta G$  value of  $-6.67$  kcal/mol and a  $K_i$  value of  $16.66 \mu\text{M}$ . Our docking results showed that neither statins nor/or ashitaba's compounds bind to residues 870–872 at the C-terminus, so neither statins nor ashitaba's compounds may be competitive with NADPH. The results of Lipinski's rule of five analysis on 15 compounds provided data on the physicochemical properties of these compounds, which may be useful in subsequent in vitro or in vivo testing. We used this RO5 as a tool to guide early-stage drug discovery.

**Supplementary Materials:** The following supporting information can be downloaded at: <https://www.mdpi.com/article/10.3390/molecules29132983/s1>, Supplementary S1. Structure of Statins Group. Supplementary S2. Lipinski Rule of Five (RO5) Hit Compound.

**Author Contributions:** Conceptualization, D.L.A., D.R. and S.M.; methodology, D.L.A. and S.M.; software, S.R.A., S.M. and M.M.; validation, D.L.A., D.R. and S.M.; formal analysis, S.R.A.; writing—original draft preparation, S.R.A.; writing—review and editing, D.L.A., D.R. and S.M.; visualization, S.R.A.; supervision, D.L.A., S.M. and M.M.; funding acquisition, D.L.A. All authors have read and agreed to the published version of the manuscript.

**Funding:** This research was funded by Universitas Padjadjaran (Riset Percepatan Lektor Kepala) to Diah Lia Aulifa No. 2203/UN6.3.1/PT.00/2022.

**Institutional Review Board Statement:** Not applicable.

**Informed Consent Statement:** Not applicable.

**Data Availability Statement:** The data generated in the present study may be requested from the first author upon reasonable request.

**Acknowledgments:** We would like to thank Universitas Padjadjaran for supporting this work and APC.

**Conflicts of Interest:** The authors declare no conflicts of interest.

## References

1. NIH. HMGCR 3-Hydroxy-3-Methylglutaryl-CoA Reductase [Homo Sapiens (Human)]. Available online: <https://www.ncbi.nlm.nih.gov/gene?Db=gene&Cmd=DetailsSearch&Term=3156> (accessed on 12 January 2023).
2. Harvard Health Publishing. How It's Made: Cholesterol Production in Your Body—Harvard Health. Available online: <https://www.health.harvard.edu/heart-health/how-its-made-cholesterol-production-in-your-body> (accessed on 9 February 2023).
3. Takei, S.; Nagashima, S.; Takei, A.; Yamamuro, D.; Wakabayashi, T.; Murakami, A.; Isoda, M.; Yamazaki, H.; Ebihara, C.; Takahashi, M.; et al.  $\beta$ -Cell-Specific Deletion of HMG-CoA (3-Hydroxy-3-Methylglutaryl-Coenzyme A) Reductase Causes Overt Diabetes Due to Reduction of  $\beta$ -Cell Mass and Impaired Insulin Secretion. *Diabetes* **2020**, *69*, 2352–2363. [[CrossRef](#)] [[PubMed](#)]
4. Islam, S.; Ahmed, K.; Al-Mamun, H.; Hoque, F. Preliminary Assessment of Heavy Metal Contamination in Surface Sediments from a River in Bangladesh. *Environ. Earth Sci.* **2015**, *73*, 1837–1848. [[CrossRef](#)]
5. Gesto, D.S.; Pereira, C.M.S.; Cerqueira, N.M.F.S.; Sousa, S.F. An Atomic-Level Perspective of HMG-CoA-Reductase: The Target Enzyme to Treat Hypercholesterolemia. *Molecules* **2020**, *25*, 3891. [[CrossRef](#)] [[PubMed](#)]
6. Shanmugam, G.; Jeon, J. Computer-Aided Drug Discovery in Plant Pathology. *Plant Pathol. J.* **2017**, *33*, 529–542. [[CrossRef](#)] [[PubMed](#)]
7. Sarver, R.W.; Bills, E.; Bolton, G.; Bratton, L.D.; Caspers, N.L.; Dunbar, J.B.; Harris, M.S.; Hutchings, R.H.; Kennedy, R.M.; Larsen, S.D.; et al. Thermodynamic and Structure Guided Design of Statin-Based Inhibitors of 3-Hydroxy-3-Methylglutaryl Coenzyme A Reductase. *J. Med. Chem.* **2008**, *51*, 3804–3813. [[CrossRef](#)] [[PubMed](#)]
8. Markowska, A.; Antoszczak, M.; Markowska, J.; Huczyński, A. Statins: Hmg-Coa Reductase Inhibitors as Potential Anticancer Agents against Malignant Neoplasms in Women. *Pharmaceuticals* **2020**, *13*, 422. [[CrossRef](#)]
9. Bitzur, R.; Cohen, H.; Kamari, Y.; Harats, D. Intolerance to Statins: Mechanisms and Management. *Diabetes Care* **2013**, *36*, S325–S330. [[CrossRef](#)]
10. Swerdlow, D.I.; Preiss, D.; Kuchenbaecker, K.B.; Holmes, M.V.; Engmann, J.E.L.; Shah, T.; Sofat, R.; Stender, S.; Johnson, P.C.D.; Scott, R.A.; et al. HMG-Coenzyme A Reductase Inhibition, Type 2 Diabetes, and Bodyweight: Evidence from Genetic Analysis and Randomised Trials. *Lancet* **2015**, *385*, 351–361. [[CrossRef](#)]
11. Cho, Y.; Choe, E.; Lee, Y.; Seo, J.W.; Choi, Y.; Yun, Y.; Wang, H.J.; Ahn, C.W.; Cha, B.S.; Lee, H.C.; et al. Risk of Diabetes in Patients Treated with HMG-CoA Reductase Inhibitors. *Metabolism* **2015**, *64*, 482–488. [[CrossRef](#)]
12. Hoogwerf, B.J. Statins May Increase Diabetes, but Benefit Still Outweighs Risk. *Clevel. Clin. J. Med.* **2023**, *90*, 53–62. [[CrossRef](#)]
13. Kusumawardhani, P.A.; Dewi, A.D.R.; Iswadi, H.; Widjaja, L.K. *Tanaman Malaikat Dari Trawas, Indonesia Ashitaba*, 1st ed.; Direktorat Penerbitan & Publikasi Ilmiah, Universitas Surabaya: Surabaya, Indonesia, 2020.
14. Battenberg, O.A.; Yang, Y.; Verhelst, S.H.L.; Sieber, S.A. Target Profiling of 4-Hydroxyderricin in *S. Aureus* Reveals Seryl-TRNA Synthetase Binding and Inhibition by Covalent Modification. *Mol. Biosyst.* **2013**, *9*, 343–351. [[CrossRef](#)] [[PubMed](#)]
15. Zhang, T.; Sawada, K.; Yamamoto, N.; Ashida, H. 4-Hydroxyderricin and Xanthoangelol from *Ashitaba (Angelica keiskei)* Suppress Differentiation of Preadipocytes to Adipocytes via AMPK and MAPK Pathways. *Mol. Nutr. Food Res.* **2013**, *57*, 1729–1740. [[CrossRef](#)] [[PubMed](#)]
16. Kim, J.H.; Son, Y.K.; Kim, G.H.; Hwang, K.H. Xanthoangelol and 4-Hydroxyderricin Are the Major Active Principles of the Inhibitory Activities against Monoamine Oxidases on *Angelica keiskei* K. *Biomol. Ther.* **2013**, *21*, 234–240. [[CrossRef](#)] [[PubMed](#)]
17. Kim, D.W.; Curtis-Long, M.J.; Yuk, H.J.; Wang, Y.; Song, Y.H.; Jeong, S.H.; Park, K.H. Quantitative Analysis of Phenolic Metabolites from Different Parts of *Angelica keiskei* by HPLC-ESI MS/MS and Their Xanthine Oxidase Inhibition. *Food Chem.* **2014**, *153*, 20–27. [[CrossRef](#)]
18. Chang, H.R.; Lee, H.J.; Ryu, J. Chalcones from *Angelica keiskei* Attenuate the Inflammatory Responses by Suppressing Nuclear Translocation of NF- $\kappa$ B. *J. Med. Food* **2014**, *17*, 1306–1313. [[CrossRef](#)] [[PubMed](#)]
19. Son, D.J.; Park, Y.O.; Yu, C.; Lee, S.E.; Park, Y.H. Bioassay-Guided Isolation and Identification of Anti-Platelet-Active Compounds from the Root of *Ashitaba (Angelica keiskei Koidz.)*. *Nat. Prod. Res.* **2014**, *28*, 2312–2316. [[CrossRef](#)] [[PubMed](#)]
20. Yasuda, M.; Kawabata, K.; Miyashita, M.; Okumura, M.; Yamamoto, N.; Takahashi, M.; Ashida, H.; Ohigashi, H. Inhibitory Effects of 4-Hydroxyderricin and Xanthoangelol on Lipopolysaccharide-Induced Inflammatory Responses in RAW264 Macrophages. *J. Agric. Food Chem.* **2014**, *62*, 462–467. [[CrossRef](#)] [[PubMed](#)]
21. Kil, Y.; Choi, S.; Lee, Y.; Jafari, M.; Seo, E. Chalcones from *Angelica keiskei*: Evaluation of Their Heat Shock Protein Inducing Activities. *J. Nat. Prod.* **2015**, *78*, 2481–2487. [[CrossRef](#)]
22. Kil, Y.-S.; Nam, J.-W.; Lee, J.; Seo, E.K. Separation of Two Major Chalcones from *Angelica keiskei* by High-Speed Counter-Current Chromatography. *Arch. Pharm. Res.* **2015**, *38*, 1506–1511. [[CrossRef](#)]
23. Kil, Y.; Kwon, J.; Lee, D.; Seo, E.K. Three New Chalcones from the Aerial Parts of *Angelica keiskei*. *Helv. Chim. Acta* **2016**, *99*, 393–397. [[CrossRef](#)]

24. Li, J.L.; Gao, L.X.; Meng, F.W.; Tang, C.L.; Zhang, R.J.; Li, J.; Luo, C.; Li, J.; Zhao, W.M. PTP1B Inhibitors from Stems of *Angelica keiskei* (Ashitaba). *Bioorganic Med. Chem. Lett.* **2015**, *25*, 2028–2032. [[CrossRef](#)] [[PubMed](#)]
25. Park, J.Y.; Ko, J.A.; Kim, D.W.; Kim, Y.M.; Kwon, H.J.; Jeong, H.J.; Kim, C.Y.; Park, K.H.; Lee, W.S.; Ryu, Y.B. Chalcones Isolated from *Angelica keiskei* Inhibit Cysteine Proteases of SARS-CoV. *J. Enzym. Inhib. Med. Chem.* **2016**, *31*, 23–30. [[CrossRef](#)] [[PubMed](#)]
26. Iimura, K.; Hattan, J.; Misawa, N.; Shindo, K. CDNA Cloning and Functional Analyses of Ashitaba (*Angelica keiskei*) Sesquiterpene Synthase Genes. *J. Oleo Sci.* **2020**, *69*, 711–718. [[CrossRef](#)] [[PubMed](#)]
27. Zhou, X.; Liang, C.; Xu, Q.; Zhang, X.; Liang, X.; Huang, Q.Y.; Su, X.J. Study on Chemical Constituents of *Angelica keiskei*. *Chin. J. Exp. Tradit. Med. Formulae* **2012**, *18*, 103–105.
28. Luo, L.; Wang, R.; Wang, X.; Ma, Z.; Li, N. Compounds from *Angelica keiskei* with NQO1 Induction, DPPH Scavenging and  $\alpha$ -Glucosidase Inhibitory Activities. *Food Chem.* **2012**, *131*, 992–998. [[CrossRef](#)]
29. Zhang, T.; Yamashita, Y.; Yasuda, M.; Yamamoto, N.; Ashida, H. Ashitaba (*Angelica keiskei*) Extract Prevents Adiposity in High-Fat Diet-Fed C57BL/6 Mice. *Food Funct.* **2015**, *6*, 135–145. [[CrossRef](#)] [[PubMed](#)]
30. Yuliantini, A.; Nurnahari, N.; Jamil, M.F.; Asnawi, A. Skrining Fitokimia Ashitaba (*Angelica keiskei*) Terhadap Enzim ACP Reduktase (InhA) Mycobacterium Tuberculosis Sebagai Senyawa Potensial Anti-TB. *Indones. Nat. Res. Pharm. J.* **2022**, *7*, 1–10. [[CrossRef](#)]
31. Muchtaridi; Yanuar, A.; Megantara, S.; Purnomo, H. *Teknik Perancangan Obat Berbantuan Komputer*; UNPAD Press: Sumedang, Indonesia, 2020.
32. Nur, M.R.F.; Oktora, S.I. Analisis Kurva Roc Pada Model Logit Dalam Pemodelan Determinan Lansia Bekerja Di Kawasan Timur Indonesia. *Indones. J. Stat. Its Appl.* **2020**, *4*, 116–135. [[CrossRef](#)]
33. Arba, M.; Arfan; Trisnawati, A.; Kurniawati, D. Pemodelan Farmakofor Untuk Identifikasi Inhibitor Heat Shock Proteins-90 (HSP-90). *J. Farm. Galen. (Galen. J. Pharm.) (e-J.)* **2020**, *6*, 229–236.
34. Rachmania, R.A. Validasi Protokol Skrining Virtual Dan Analisis Interaksi Inhibitor Antiproliferasi Sel Kanker Berbasis Bahan Alam Terhadap Reseptor Cyclin-Dependent Kinase 4 (Cdk 4). *Media Farm. J. Ilmu Farm.* **2019**, *16*, 21. [[CrossRef](#)]
35. Istvan, E.S.; Deisenhofer, J. Structural Mechanism for Statin Inhibition of HMG-CoA Reductase. *Science* **2001**, *292*, 1160–1164. [[CrossRef](#)] [[PubMed](#)]
36. Istvan, E.S.; Palnitkar, M.; Buchanan, S.K.; Deisenhofer, J. Crystal Structure of the Catalytic Portion of Human HMG-CoA Reductase: Insights into Regulation of Activity and Catalysis. *EMBO J.* **2000**, *19*, 819–830. [[CrossRef](#)] [[PubMed](#)]
37. Costa, C.H.S.; Oliveira, A.R.S.; Dos Santos, A.M.; da Costa, K.S.; Lima, A.H.L.E.; Alves, C.N.; Lameira, J. Computational Study of Conformational Changes in Human 3-Hydroxy-3-Methylglutaryl Coenzyme Reductase Induced by Substrate Binding. *J. Biomol. Struct. Dyn.* **2019**, *37*, 4374–4383. [[CrossRef](#)]
38. Carter, A.A.; Gomes, T.; Camacho, X.; Juurlink, D.N.; Shah, B.R.; Mamdani, M.M. Risk of Incident Diabetes among Patients Treated with Statins: Population-Based Study. *BMJ* **2013**, *346*, f2610. [[CrossRef](#)] [[PubMed](#)]
39. Aziz, F.K.; Nukitasari, C.; Oktavianingrum, F.A.; Aryati, L.W.; Santoso, B. Hasil In Silico Senyawa Z12501572, Z00321025, SCB5631028 Dan SCB13970547 Dibandingkan Turunan Zerumbon Terhadap Human Liver Glycogen Phosphorylase (115Q) Sebagai Antidiabetes. *J. Kim. Val.* **2016**, *2*, 120–124. [[CrossRef](#)]
40. Santoso, B. Profil Sebaran Hasil Idock Untuk Kelompok Senyawa Aktif, Decoys, Dan ZINC-Induser Terhadap Protein PPAR-Gamma. In Proceedings of the 5th University Research Colloquium (URECOL), Yogyakarta, Indonesia, 18 February 2017; pp. 1254–1259.
41. Mysinger, M.M.; Carchia, M.; Irwin, J.J.; Shoichet, B.K. Directory of Useful Decoys, Enhanced (DUD-E): Better Ligands and Decoys for Better Benchmarking. *J. Med. Chem.* **2012**, *55*, 6582–6594. [[CrossRef](#)] [[PubMed](#)]
42. Liliana; Istyastono, E.P. Uji in silico senyawa 2,6-dihidroksiantraquinon sebagai ligan pada reseptor estrogen alfa. *J. Famasi Sains Dan Komunitas* **2015**, *12*, 76–79.
43. Jiang, S.-Y.; Li, H.; Tang, J.-J.; Wang, J.; Luo, J.; Liu, B.; Wang, J.-K.; Shi, X.-J.; Cui, H.-W.; Tang, J.; et al. Discovery of a Potent HMG-CoA Reductase Degrader That Eliminates Statin-Induced Reductase Accumulation and Lowers Cholesterol. *Nat. Commun.* **2018**, *9*, 5138. [[CrossRef](#)]
44. Vögeli, B.; Shima, S.; Erb, T.J.; Wagner, T. Crystal Structure of Archaeal HMG-CoA Reductase: Insights into Structural Changes of the C-Terminal Helix of the Class-I Enzyme. *FEBS Lett.* **2019**, *593*, 543–553. [[CrossRef](#)]
45. Benet, L.Z.; Hosey, C.M.; Ursu, O.; Oprea, T.I. BDDCS, the Rule of 5 and Drugability. *Adv. Drug Deliv. Rev.* **2016**, *101*, 89–98. [[CrossRef](#)]
46. Kilo, A.L.; Aman, L.; Sabihi, I.; Kilo, J. Studi Potensi Prazolin Tersubstitusi 1-N Dari Tiosemikarbazon Sebagai Agen Antiamuba Melalui Uji in-Silico. *Indones. J. Chem.* **2019**, *7*, 9–16.
47. Naufa, F.; Mutiah, R.; Yen, Y.; Indrawijaya, A. Studi in Silico Potensi Senyawa Katekin Teh Hijau (*Camellia Sinensis*) Sebagai Antivirus SARS CoV-2 Terhadap Spike Glycoprotein (6LZG) Dan Main Protease (5R7Y). *J. Food Pharm. Sci.* **2022**, *2022*, 584–596. [[CrossRef](#)]

- 
48. Lipinski, C.A. Lead- and Drug-like Compounds: The Rule-of-Five Revolution. *Drug Discov. Today Technol.* **2004**, *1*, 337–341. [[CrossRef](#)]
  49. Lipinski, C.A.; Lombardo, F.; Dominy, B.W.; Feeney, P.J. Experimental and Computational Approaches to Estimate Solubility and Permeability in Drug Discovery and Development Settings. *Adv. Drug Deliv. Rev.* **2012**, *64*, 4–17. [[CrossRef](#)]

**Disclaimer/Publisher’s Note:** The statements, opinions and data contained in all publications are solely those of the individual author(s) and contributor(s) and not of MDPI and/or the editor(s). MDPI and/or the editor(s) disclaim responsibility for any injury to people or property resulting from any ideas, methods, instructions or products referred to in the content.